Short Window Intra-Spacecraft RFID Localization

Sournav Sekhar Bhattacharya, Lazaro "Danny" Rodriguez, Patrick Fink
NASA Johnshon Space Center - EV 111
Houston, USA
sournavsekhar.bhattacharya@nasa.gov, lazaro.d.rodriguez@nasa.gov

***Abstract*—Logistics management has emerged as a key component to activites conducted in space. The RFID Enabled Autonomous Logistics Management (REALM) system has played a key role in providing cargo tracking capabilities in the noisy environment of the ISS. Currently, the inferencing engines used by REALM to predict the location of RFID tagged items operate on an hour of data. Movements aboard space stations occur on the scales of seconds. In this work we propose a new inferencing engine, that produces an embedding space that represents the location of RFID marked cargo on the scale of 30 seconds to 2 minutes of data, allowing for the categorization of movement of cargo, and predictions of a coarse location in less time than existing engines. [3], [4]**

***Index Terms*—Unsupervised Machine Learning, RFID Localization, Space**

I. Introduction

The cataloging and tracking of cargo and supplies aboard space stations such as the ISS with RFID systems has become paramount to mission success. The small interiors of space stations (such as the ISS) coupled with their metallic construction offer a highly noisy environment for RFID systems. Currently the inferencing engines and use large models that require large compute resources to train. The approach discussed utilizes more basic unsupervised machine learning elements (such as SVD), that require fewer computing resources than existing systems. [3], [5]

II. Methodology

A. Virtual Antenna

In our experimental set up we use linearly polarized antennas, each polarized on 50 different frequencies. For a given period of time each antenna may have several RFID readings, but these will be distributed along different polarities. If a target RFID tag and an antenna are similarly polarized then the chance that the tag is read by the antenna is higher. Due to the dependance on signal strength on polarization grouping tag reads by antenna alone may lead to erronous conclusions about the tags proximity to an antenna. Thus we suggest a virtual antenna, which is an antenna and frequency pairing. For n linearly polarized antennas, which are polarized along m frequencies, there are a total of $n \times m$ different virtual antennas.

B. Dual Antenna Plot

A dual antenna plot is a vizualization of the RFID data gathered by virtual antennas. If there are n virtual antennas, then a dual antenna plot D will have the dimensions $n \times n$. Each element D_{ij} where $i < k$, and $j < k$ is defined as follows:

$$D_{ij} = \begin{cases} 1, & \text{tag read on virtual antennas } i \text{ and } j \\ 0 & \text{otherwise} \end{cases}$$

In this case the ordering of virtual antennas is important, we consider $antenna\ major\ ordering$. This is when virtual antennas, belonging to the same physical antenna are grouped together. These physical antenna groups are then ordered based on local proximity. In order to find this ordering, we construct a computational graph, $G = (V, E)$, where nodes $v \in V$ correspond to physical antennas, and edges $e \in E$ correspond to the distances between antennas. A greedy search is conducted in this graph starting from one of the antennas in the pair $x, y \in V$ such that $e_{xy} = max(E)$.

Since the x and y axes both correspond to the same set of virtual antennas, only half of the total elements in the DAP are used, split along the diagonal. In order to avoid repition, we define the

Trade names and trademarks are used in this report for identification only. Their usage does not constitute an official endorsement, either expressed or implied, by the National Aeronautics and Space Administration

Algorithm 1 Algorithm to find ordering of physical antennas

$G = (V, E)$
$v_{curr} = max(E)$
exp= ϕ
Order= ϕ
while Order.length != $|V|$ **do**
  $e_{min} = MAX$
  $v_{min} = NULL$
  for v_i in v_{curr}.neighbors **do**
    if $v_i \notin$ exp and $e(v_{curr}, v_i) < e_{min}$ **then**
      v_{min} = v_i
      e_{min} = $e(v_{curr}, v_i)$
    end if
  end for
  Order.push(v_{min})
  Explored.push(v_{min})
  $v_{curr} = v_{min}$
end while
return Order

time shifted DAP, for a fixed collection of tags T, for a time period t_k, where D_{ij} is defined as follows given V is the set of virtual antennae:

$$D_{ij} = \begin{cases} 1, T \text{ read by } V_i \wedge V_j,\ i \geq j \text{ at } t_k \\ 0, T \text{ not read by } V_i \wedge V_j,\ i \geq j \text{ at } t_k \\ 1, T \text{ read by } V_i \wedge V_j,\ j > i \text{ at } t_{k-1} \\ 0, T \text{ not read by } V_i \wedge V_j,\ j > i \text{ at } t_{k-1} \end{cases}$$

Using time shifted dual antenna plots allows us to present two adjascent frames of data on a single plot. Our approaches to the localization task, or movement detection task use the dual antenna plot as an aggregated data sample organized by virtual antennas. This data augmentation step allows for an intermediate output of the localization pipeline that is interperable by humans, and also reduces the effort on the machine learning portions of the pipeline to derive the relationship between rifd readings, antenna IDs, and frequency.

We do not consider the RSSI value, or phase of readings gathered, but rather only focus on the occurence of a reading between two virtual antennas. This is because our target environments (ISS, Wireless Testbed) are constructed from metal, and introduce noise into RSSI via multipath.

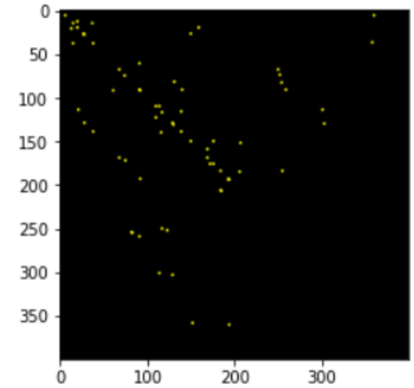

Fig. 1. Example of a time shifted dual antenna plot

C. Singular Value Decomposition

Given a matrix $X \in \mathbb{R}^{n\times d}$, the singular value decomposition theorem states that there must exist a decomposition $X = U\Sigma V^T$, where $U \in \mathbb{R}^{n\times n}$, $\Sigma \in \mathbb{R}^{n\times d}$, and $V \in \mathbb{R}^{d\times d}$. Additionally, U, V are orthogonal matrices, while Σ is a diagonal matrix where $\forall x \in \Sigma, x \geq 0$.

Note that for a singular value decomposition, $X = U\Sigma V^T$:

$$XX^T = U\Sigma V^T V \Sigma^T U^T = U\Sigma\Sigma^T U^T = U\Sigma^2 U^T.$$

We can observe that this is just an eigen decomposition of XX^T. Thus to compute U and Σ we need to compute the eigenvectors of XX^T, and the square root of the eigenvalues of XX^T. Similarly for $X^T X$ we get:

$$X^T X = V\Sigma^T U^T U \Sigma V^T = V\Sigma^T\Sigma V^T = V\Sigma^2 V^T$$

Thus to compute V we must compute the eigenvectors of $X^T X$. Note that this means the eigenvalues of $X^T X$ and XX^T must be the same.

In this work we are interested in using SVD for dimensionality reduction. This can be done by considering the truncated SVD. The truncated SVD for a matrix $X \in \mathbb{R}^{n\times d}$ with SVD, $U\Sigma V^T$ is computed by choosing a value $r < d$, and truncating the SVD. This is done by only considering the first r columns of U, the first r terms in the diagonal of Σ, and the first r rows of V^T. The resultant matrix is a compressed version of the matrix X of rank r, furthermore the matrix $U\Sigma$ is a dense matrix corresponding to the principle components of the input X. Since $V^{-1} = V^T$ because V is orthogonal, $XV^{T^{-1}} = X(V^T)^T = XV = U\Sigma$.

In our work we use the scikit learn library with a randomized SVD algorithm. This algorithm approximates V using an iterative approach, where an increased accuracy is achieved by increasing the number of iterations. This V, can be thought of as a "learned model" where a series of n records each of dimension d is combined to produce a matrix $X_{training}$ for which V is calculated. Then during the testing phase a matrix X_{test} with k records each of dimension d can be multiplied with V to arrive at a truncated matrix $X'_{test} \in \mathbb{R}^{k \times r}$. [1]

D. Constructing an Embedding Space

The input dual antenna plots for our given antenna setup are of dimension 400×400. This means there are $160,000$ pixels to consider when conducting a statiscal analysis. Additionally the data is observed to be sparse, since the time windows at which this system is used is on the scale of $30-200$ seconds, meaning that there are few chances for a limited group of tags to be read by the antennae. We propose the use of a truncated SVD to reduce the dimensionality of the dual antenna plot. Since we use an iterative approach to approximate the singular value decomposition, such that the right singular matrix V is approximated from the input matrix X, we construct a "training" X that can be used to compute the right singular matrix. The product of the matrix X and the right singular matrix V will approximate the principle components of the data. The training matrix X is constructed by taking a set of d dual antenna plots (DAPs), and flattening each DAP to a single 160,000 dimension vector. The rows of X will be these vectors, and the DAPs they correspond to, represent RFID data gathered from "marker tags". These are tags that are fixed in known location along the walls of the testbed or target environment. These tags are assumed to never move. Aside from the initial installation of the marker tags there is no human intervention needed in the gathering of the training data. Once the training matrix X is constructed, we compute an approximate SVD on this matrix. We take the right singular matrix V that is computed and store it as our model. The image space of V is considered the embedding space. During inference, we take the flattened dual antenna plots and multiply them with the right singular matrix V to arrive at a particular point in the embedding space. [1]

Since the approach is iterative we observed that to arrive at an embedding space of single dimension was too computationally intensive for our computer system. Instead we arrived at a ten dimensional embedding space first, and saved the right singular matrix from this approximation. Then we conducted a second SVD approximation going from the ten dimensional embedding space to a single dimensional embedding space. Moving to a single dimensional embedding space greatly reduced the amount of data needed to express the data in the DAP to just a single floating point number. [1]

E. Virtual Bags

Note that our embedding space is the image space of the trained right singular matrix. The input to the SVD process that arrives at the right singular matrix is a training set X, where each row $x \in X$ is a flattened Dual Antenna Plot (DAP) corresponding to a collection of marker tags. However through experimentation it was found that taking a random collection of marker tags to produce the dual antenna plot produces an embedding space where the position of a point on the embedding space does not correlate to any spatial position in the physical world. This is because on inference we consturct our dual antenna plot for RFID tags present inside or around a single cargo transfer bag (CTB). Marker tags that are place on the testbed or target location may be placed in rows or columns to gain maximum coverage, whereas tags present in a bag are physically closer to one another and may have a greater diversity in orientation. This effects the RF characteristics displayed by the RFID tags. As a result we propose the use of "virtual bags". These are groupings of marker tags. In particular marker tags are said to belong to the same "virtual bag" if they are within a user defined threshold distance to a source tag, and if they have above a certain threshold of readings within the time period of interest. Note that each virtual bag has a single source tag, and a certain "size". This "size" is the maximum number of tags that can be in one virtual bag. It was seen that to get a similar number of readings to actual bags the size of the time window of the DAPs corresponding to the virtual bags was larger ($250-300$ seconds as opposed to $30-200$ seconds).

F. Embedding Space after Virtual Bags

The resulting embedding space that was arrived to was much more closely correlated to the spatial position of the bag in the testbed. Furthermore this

Fig. 2. Internal panoramic view of testbed. 1: Cargo Transfer Bag (CTB), 2: Wooden podium, 3: Metal framed chair, 4: Marker tags for training, 5: RFID Reader Antenna, 6: Sample metallic floor tile

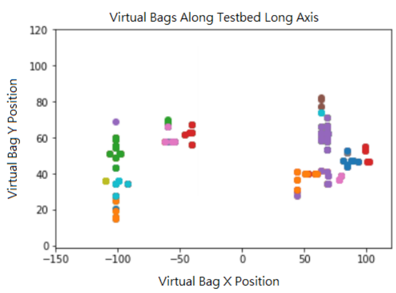

Fig. 3. Virtual bags along the long axis of the testbed, each color group is a different virtual bag

approach only uses training data gathered from virtual bags which do not require human intervention during their operation. Since the RF environment of a particular target location may change over time the system can be retrained periodically without any human intervention.

III. Experimental Setup

The testbed is a cylindrical chamber with a raised metal floor. The floor is split into a series of nine square metallic tiles of dimension $60.75cm \times 60.75cm$. Although there are a total of 10 antenae present in the testbed, for this work, only 8 were used. Specifically, there were four antenae on each end of the testbed along the long axis. Each group of 4 antennas is connected to areader device, which schedules the usage of antennas. For the experiments conducted in this work, each antenna connected to a reader was turned on for 1 second in round robin fashion. The walls on which the marker tags are present are not reflective for RF purposes, thus reflections occur at the metal walls of the cylidrical chamber. The physical set up of this system is representative of a module on the international space station in order to recreate a highly reflective RF environment. The system was placed in session 0, since they key goal of the engine proposed is to estimate location.

In order to test both movement and localization representation capabilities of the embedding space, two different types of experiments are considered. The first is a localization experiment. Here we take a CTB (cargo transfer bag) and place it above each tile for five minutes. In our experiments we used both a wooden pedastal, and a metal framed chair to seperate the bag from the metallic floor. The second type of experiment is similar in that both a wooden podium and metal chair are used to provide seperation between the floor tiles and the CTB. However, to see how movements would translate into the embedding space, the CTB was moved-from tiles closer to one end of the testbed, to those at the far end of the testbed and back to the middle. The movements themselves were rapid and occured over a time frame of 3-5 seconds, however between subsequent movements a larger time gap (on the order of 1-3 minutes) was used. For variations in the number of tags used, the top k performing tags are chosen, where performance is determined by the number of times a particular tag was read.

IV. Results

The two aims of this localization engine are to predict a coarse location of a CTB (cargo transfer bag), and to predict when movement occurs and in which direction.

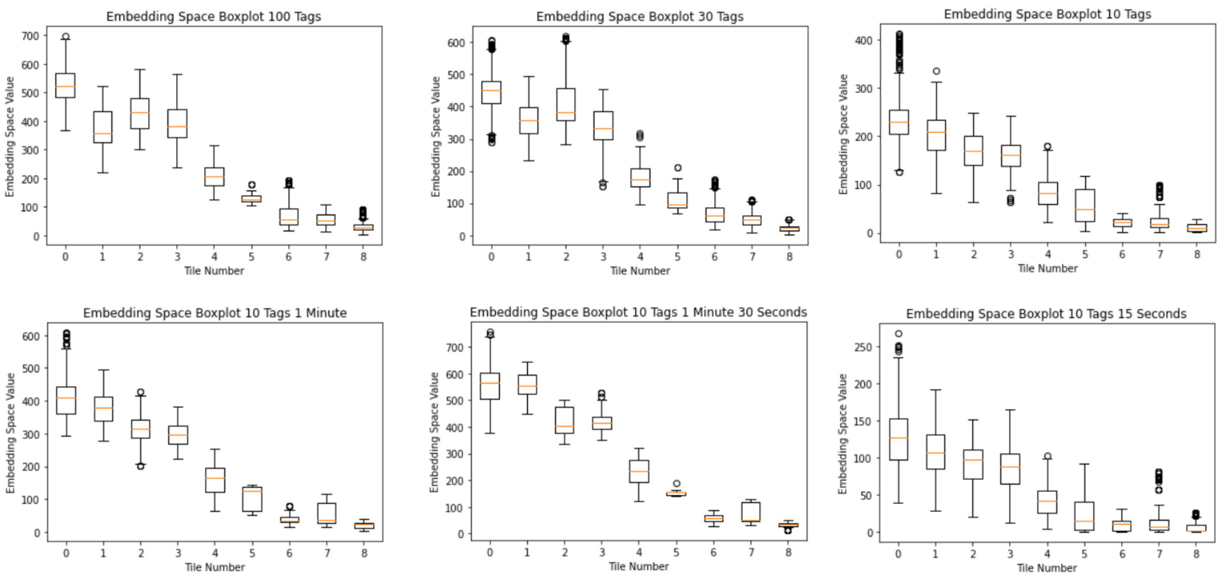

Fig. 4. Embedding space represented as a box plot using 120 tags in a 30 second window

A. *Static Coarse Localization*

The localization experiment is aimed at testing the capabilities of the system to predict locations when a given CTB is not moving. The "scale" of the embedding space for a particular set of dual antenna plots can be defined as the distance between the mean of data collected on tile 0 and the mean of all data collected on tile 9. It can be seen that as the number of tags considered in the dual antenna plot, the scale of the embedding space also decreases. As the time slice considered for the dual antenna plot increases, the scale of the embedding space also increases. A smaller scale embedding space means that for a given set of tags the seperability between tiles reduces.

The number of outliers for each tile also decreases with both an increase in the number of tags present in the dual antenna plot, or the time window considered. It is also observed that the variance around the mean for each box plot reduces as the time window considered for the dual antenna plot increases.

A larger time window means that more antenna cycles are considered, and more tags can be read. A larger number of tags increases the likelihood that the tags read by any given antenna, belong to the subset considered. In either case, the number of tag reads increases. Thus, the number of tag

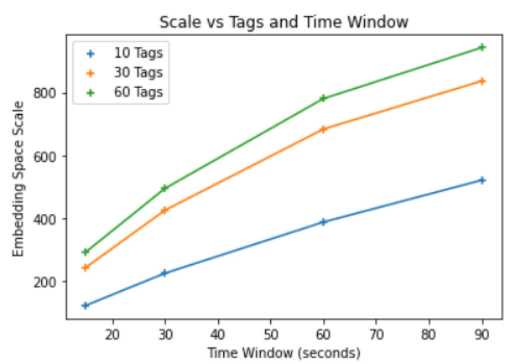

Fig. 5. Embedding scale vs the number of tags present and time window

reads present in a dual antenna plot determine the seperability of the data within the embedding space.

It was seen that the difference between embedding space scales, and overall quality of results was same regardless of the position in the z axis, and the material on which the CTB rested (wooden pedestal, or metal framed chair).

B. *Movement*

In the movement test, the CTB moves from tile 8 to tile 0 and then to tile 4 after a pause. The "dual antenna plot sequence" is the collection of dual antenna plots ordered by the start of their

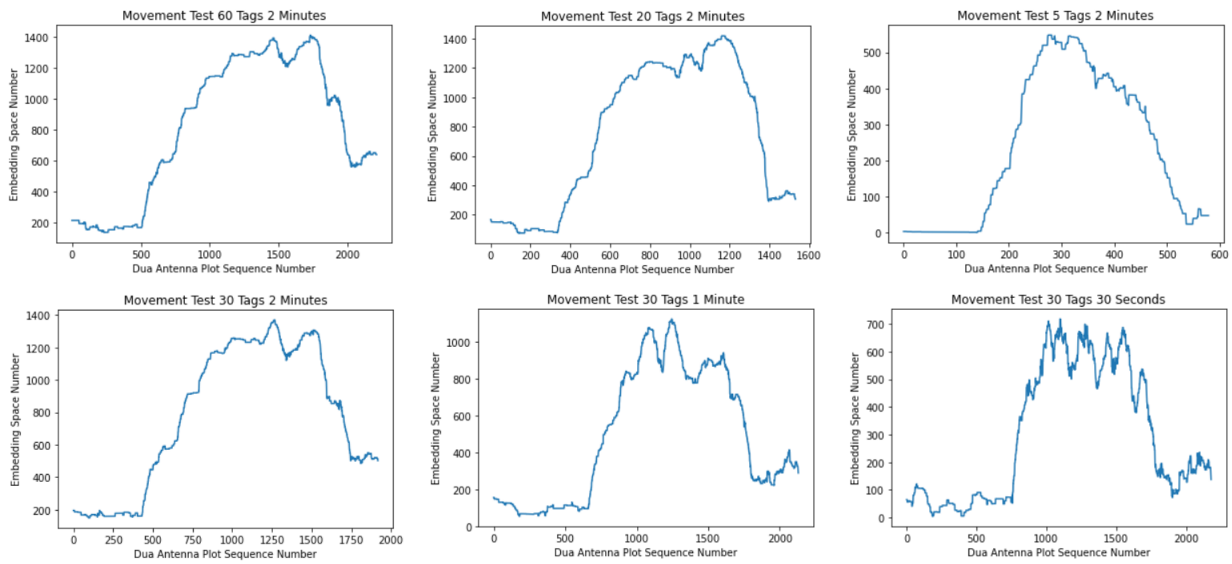

Fig. 6. Embedding space represented as a box plot using 120 tags in a 30 second window

time window, and the dual antenna plot sequence number is the position of the dual antenna plot in that sequence. If the sequence number of a particular dual antenna plot x is larger than another y, then data in x corresponds to a time after the data in y. Thus the dual antenna plot sequence number is a measure of time.

The movement test shows that using a larger time window within the dual antenna plot allows for an embedding space prediction that is more closely related to tile position. Reducing the time window results in a coarser relationship between the embedding space number and the actual physical position of the CTB along the long axis of the testbed. Furthermore, reducing the number of tags reduces the embedding space scale as well as the accuracy of the embedding space. With a small number of tags and a shorter time window only a coarse estimate (which half of the testbed) can be made about where the CTB is along the long axis due to greater noise in a smaller scale embedding space.

V. Conclusion

Formulating a dual antenna plot (DAP) to represent RFID data, and using the singular value decomposition method to compress the DAP into an embedding space allows for a computationally cheap method to localize RFID tags, while working on limited data. While this was tested in an analog comparable to an ISS module, the future direction of this work aims at testing it on board the ISS itself.

References

[1] V. Klema and A. Laub, ”The singular value decomposition: Its computation and some applications,” in IEEE Transactions on Automatic Control, vol. 25, no. 2, pp. 164-176, April 1980, doi: 10.1109/TAC.1980.1102314.

[2] F. Pedregosa et al. , ”Scikit-learn: Machine Learning in Python”, 2018, https://doi.org/10.48550/arXiv.1201.0490

[3] J. Simonoff, J. Berger, A. Abdulali, O. Lerner, L. D. Rodriguez and P. Fink, ”Intra-Spacecraft RFID Localization,” 2021 IEEE International Conference on RFID (RFID), Atlanta, GA, USA, 2021, pp. 1-8, doi: 10.1109/RFID52461.2021.9444373.

[4] Fink, Patrick, and John'Jack James. ”RFID Enabled Autonomous Logistics Management”. No. JSC-CN-36716. 2016.

[5] T. F. Kennedy, R. S. Provence, J. L. Broyan, P. W. Fink, P. H. Ngo and L. D. Rodriguez, ”Topic models for RFID data modeling and localization,” 2017 IEEE International Conference on Big Data (Big Data), Boston, MA, USA, 2017, pp. 1438-1446, doi: 10.1109/BigData.2017.8258077.